SIMULATIONS OF TARGETS FOR NDCX II*

J. J. Barnard[1], J. Armijo[2], F. M. Bieniosek[2], A. Friedman[1], M. Hay[2], E. Henestroza[2], B.G. Logan[2], R. M. More[2], P. A. Ni[2], L. J. Perkins[1], S. F. Ng[2,4], S. A. Veitzer[3], J. S. Wurtele[2], S. S. Yu[2,4], A. B. Zylstra[2]

1. Lawrence Livermore National Laboratory, Livermore, CA 94550, USA
2. Lawrence Berkeley, National Laboratory, Berkeley, CA 94720 USA
3. Tech-X Corporation, Boulder, CO 80303 USA
4. Chinese University, Hong Kong, China

Twelfth US-Japan Workshop on Heavy Ion Fusion and High Energy Density Physics

San Francisco, CA

September 6 – 11, 2009

*Work performed under the auspices of the U.S. Department of Energy under contract DE-AC52-07NA27344 at LLNL, and University of California contract DE-AC02-05CH11231 at LBNL

NDCX II will serve as a platform for warm dense matter experiments and as a test bed for heavy ion fusion

1. Experimental concepts for Warm Dense Matter (WDM)

   a. planar solid targets
   b. metallic foams
   c. cylindrical "bubbles"
   d. spherical bubbles

2. Connecting simulations of WDM targets to diagnostics

   a. simulating brightness temperature at critical density point
   b. simulating velocity at critical density point

3. Simulations of experiments relevant to Heavy Ion Fusion (HIF)

   a. coupling physics: two-pulse/ ramped pulse experiments

Complementary oral talks at IFSA cover other aspects of NDCX I and NDCX II

Oral 3.8.1 Frank Bieniosek, Wednesday, 9/9, 3:00 pm
ION-BEAM-DRIVEN WARM DENSE MATTER EXPERIMENTS

Oral 3.8.2 Alex Friedman, Wednesday, 9/9, 3:20 pm
PHYSICS DESIGN FOR NDCX-II, A SHORT-PULSE ION BEAM DRIVER FOR NEAR-TERM WDM AND TARGET PHYSICS STUDIES

NDCX I is laying the groundwork for NDCX II

NDCX I

0.35 MeV,

0.003 μC

Now

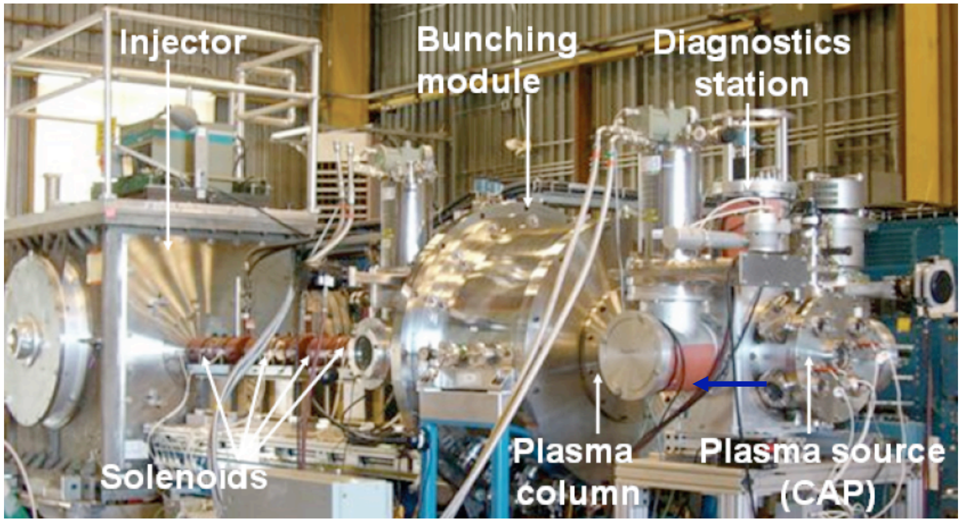

- **Explore metal liquid/vapor boundaries at T ~ 0.4 eV**
- **Evaporation rates/ bubble and droplet formation**
- **Test beam compression physics**
- **Test diagnostics**

NDCX II

3 - 6 MeV,

0.03 μC

Completion date: 2011

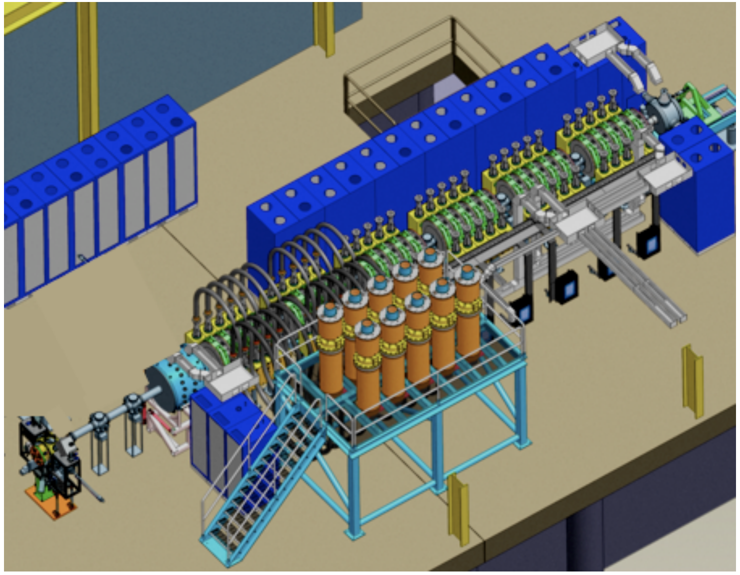

- **Bragg peak (uniform) heating**
- **T ~1-2 eV in planar metal targets (higher in cylindrical/spherical implosions)**
- **Ion$^+$/Ion$^-$ plasmas**
- **Critical point; complete liquid/ vapor boundary**
- **Transport physics (e-cond. etc)**
- **HIF coupling and beam physics**

Several target options have been considered for WDM studies on NDCX II

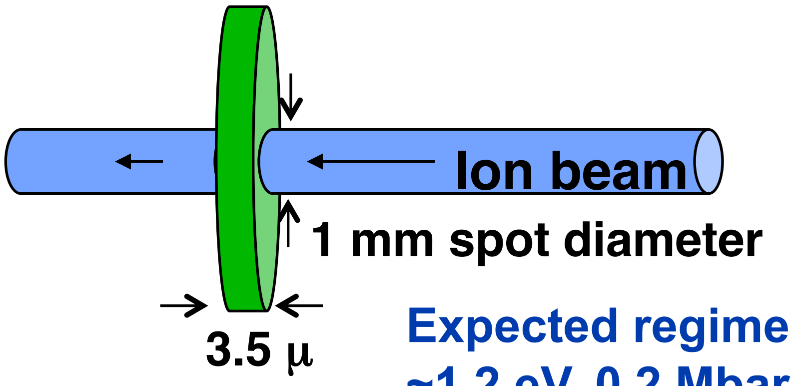

Expected regime:
~1.2 eV, 0.2 Mbar

Solid planar targets

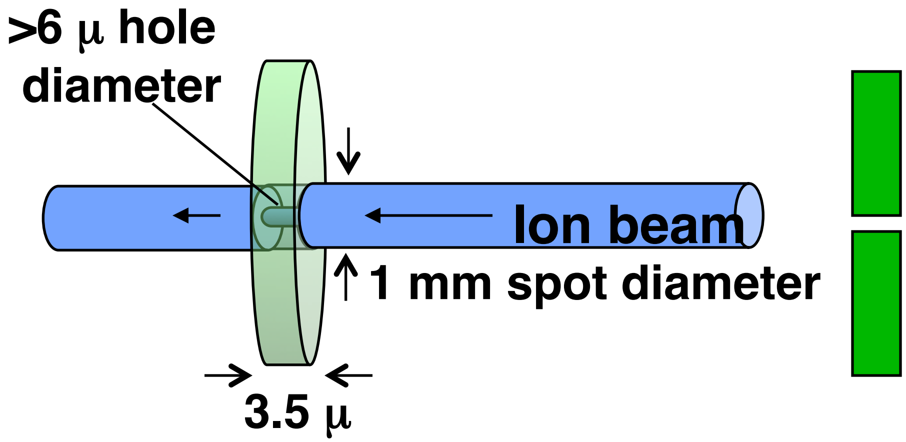

Cylindrical "bubble" targets

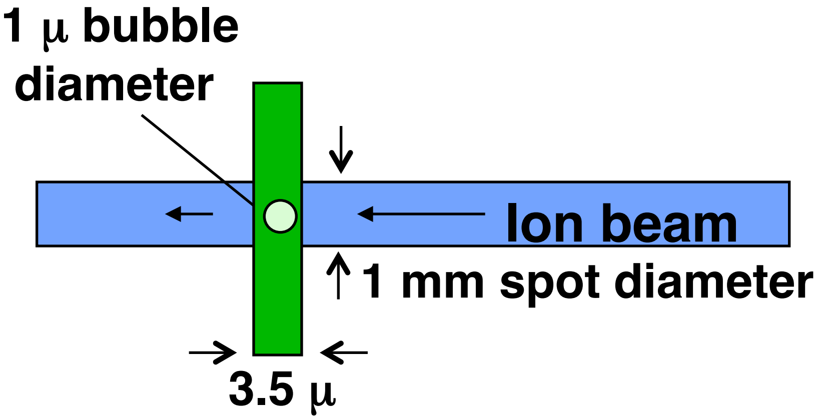

Spherical bubble targets

Foam densities
~ few % to solid

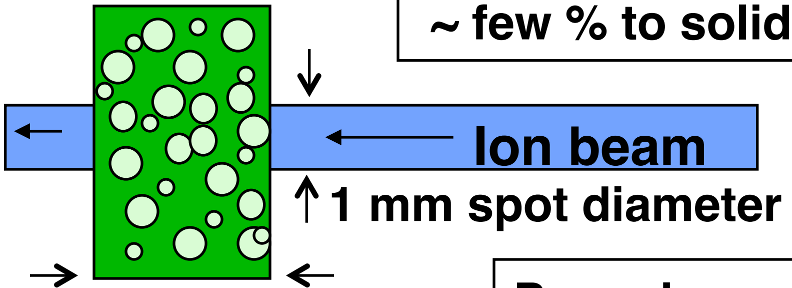

(for 10% foam)

Pore size
~ nm to ~ μm

Foam planar targets

The nominal beam assumes a 30 J/cm^2 2.8 MeV Li ion beam, corresponding to 20 kJ/g in Al (SRIM)

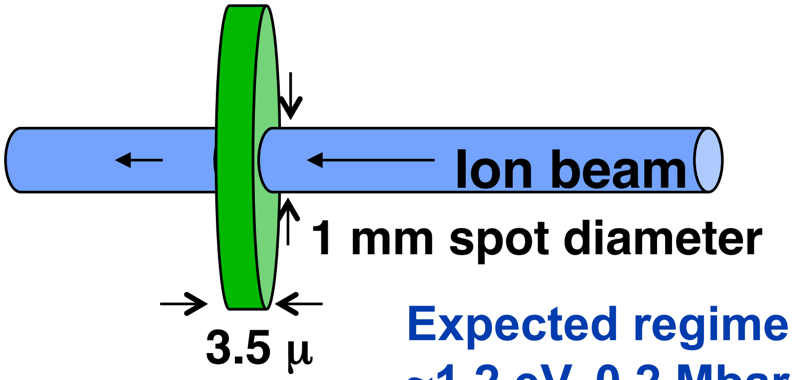

Expected regime:
~1.2 eV, 0.2 Mbar

Solid planar targets

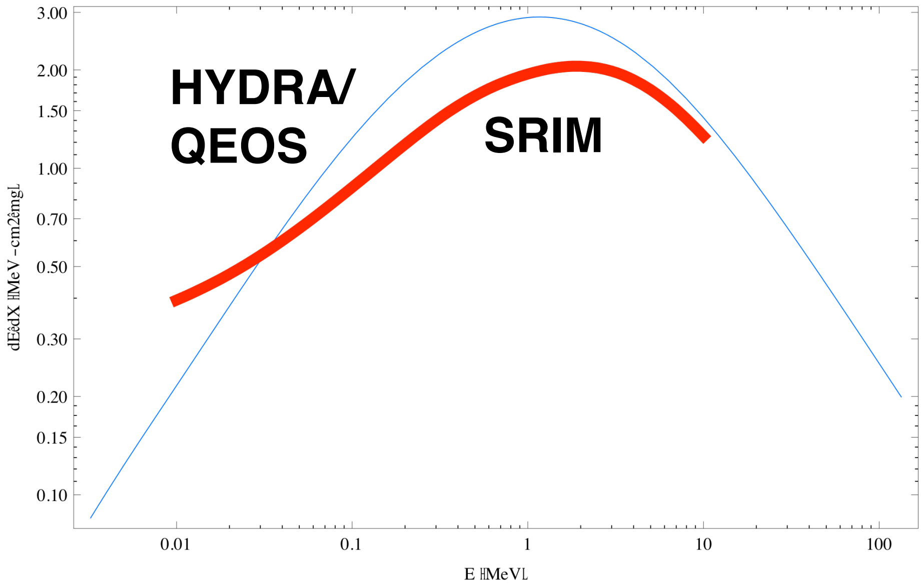

For HYDRA[1] runs we assume the nominal beam results in 20 kJ/g in Al. This implies the simulated beam had a fluence of 20 J/cm^2 (instead of 30 J/cm^2)

---

[1] **M. M. Marinak, G. D. Kerbel, N. A. Gentile, O. Jones, D. Munro, S. Pollaine, T. R. Dittrich, and S. W. Haan, Phys. Plasmas 8, 2275 (2001).**

An example of two significantly different EOS

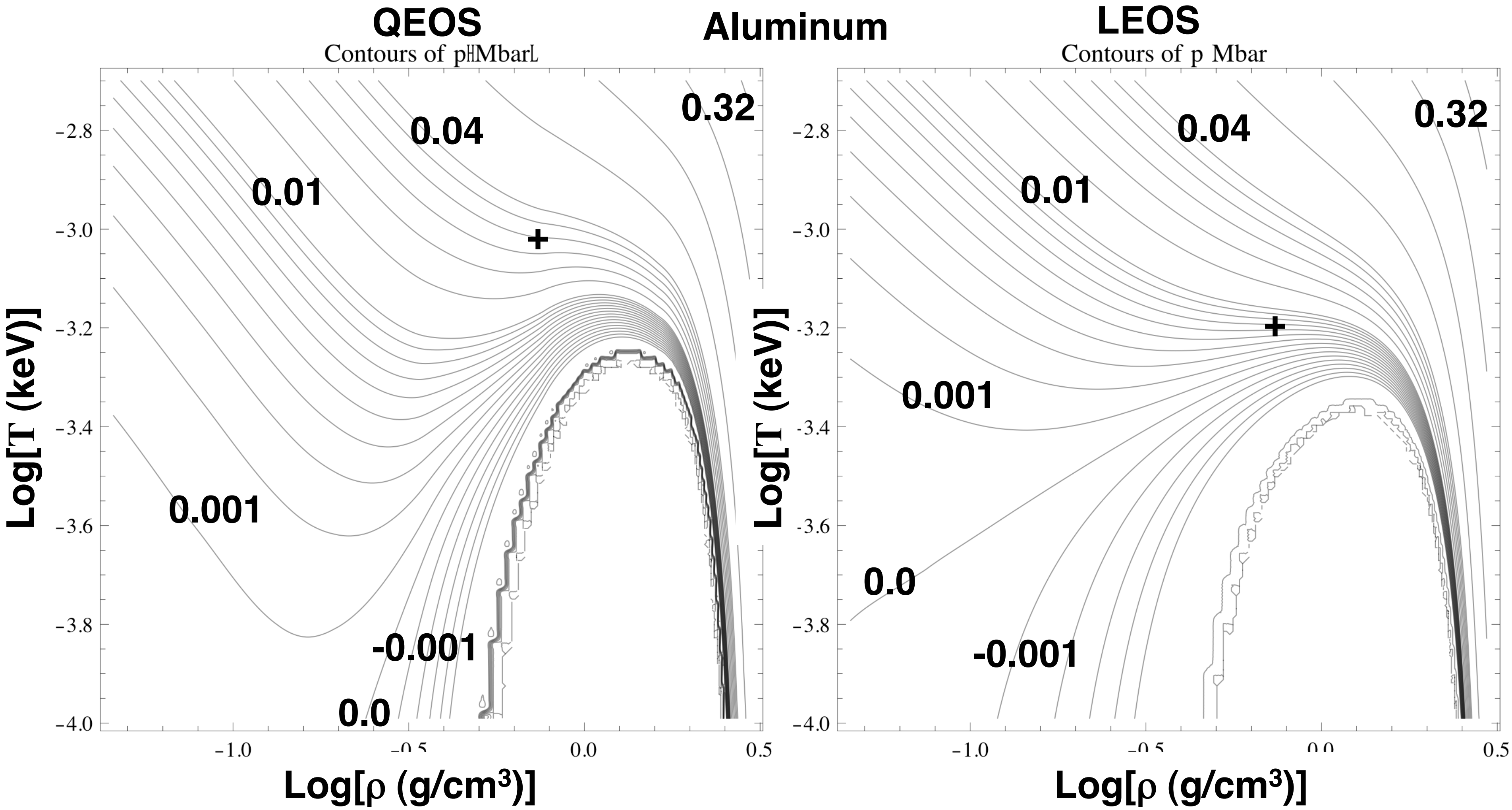

Critical point:
p=0.029 MBar
ρ=0.78 g/cm^3
T=0.945 eV

Theories and experiments place critical point between 5500 K and 12000 K (0.5 eV and 1.0 eV)

Critical point:
p=0.0065 MBar
ρ=0.70 g/cm^3
T=0.633 eV

Evolution of center of 3.5 μ thick Al foil over the heating phase (1 ns) using QEOS without maxwell construction

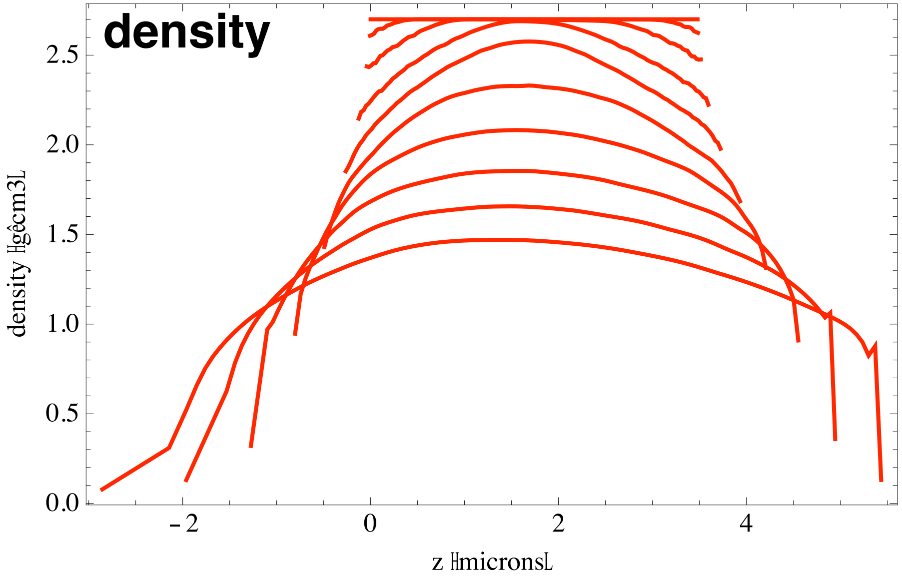

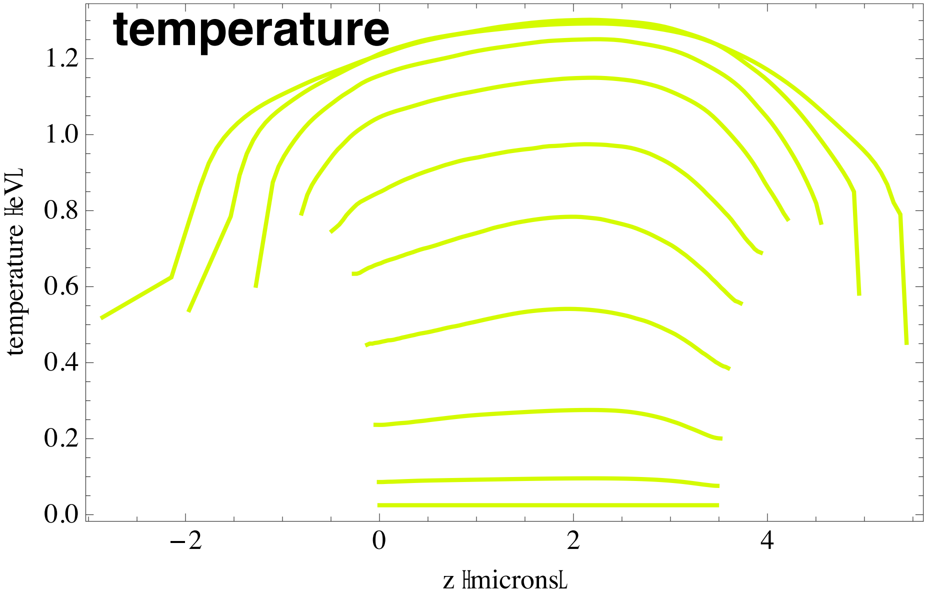

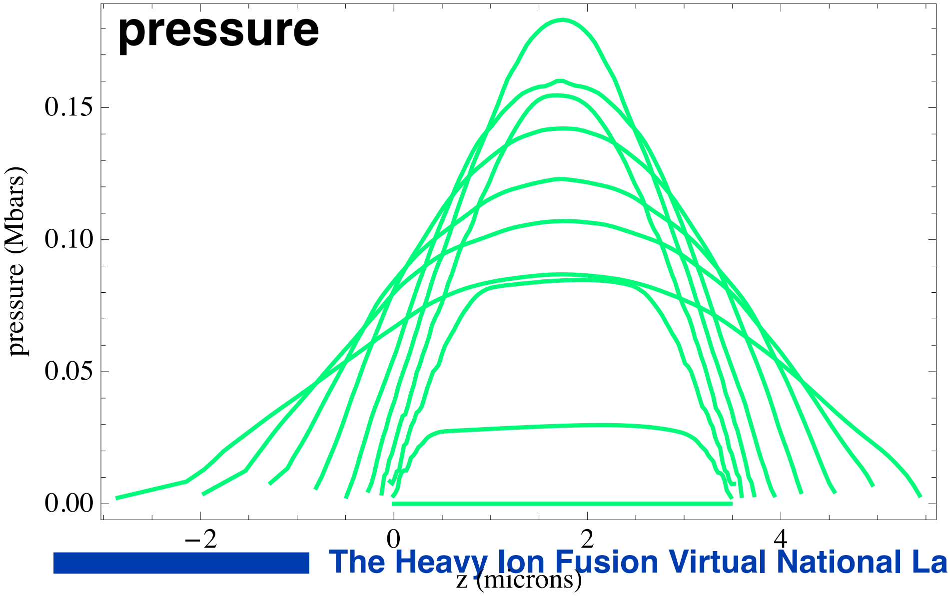

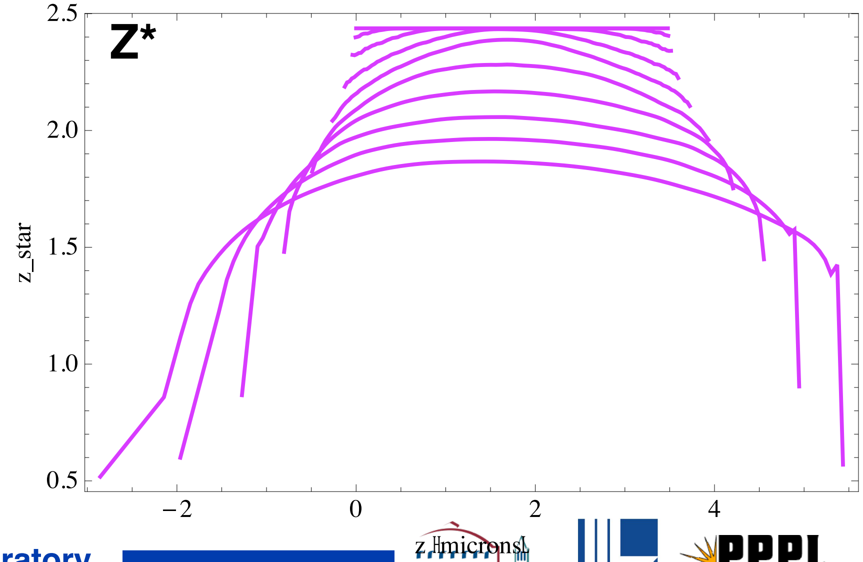

Evolution of center of 3.5 μ thick Al foil over the heating phase (1 ns) using QEOS without maxwell construction

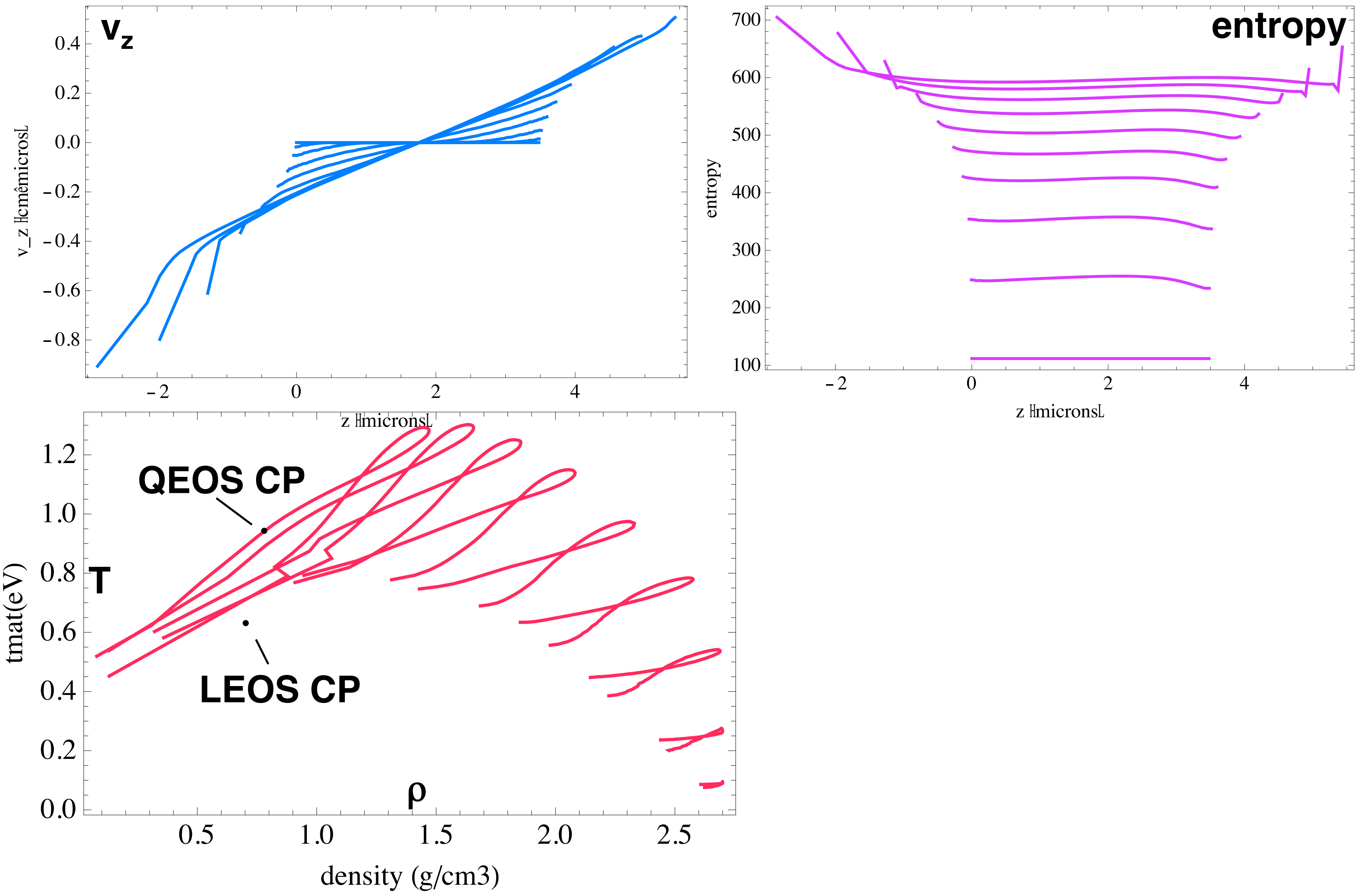

Target evolution was tracked for 30 ns

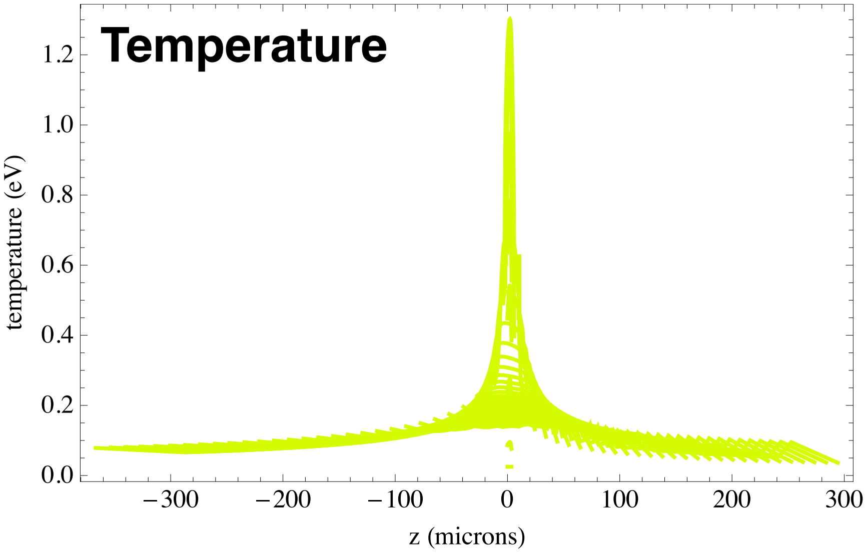

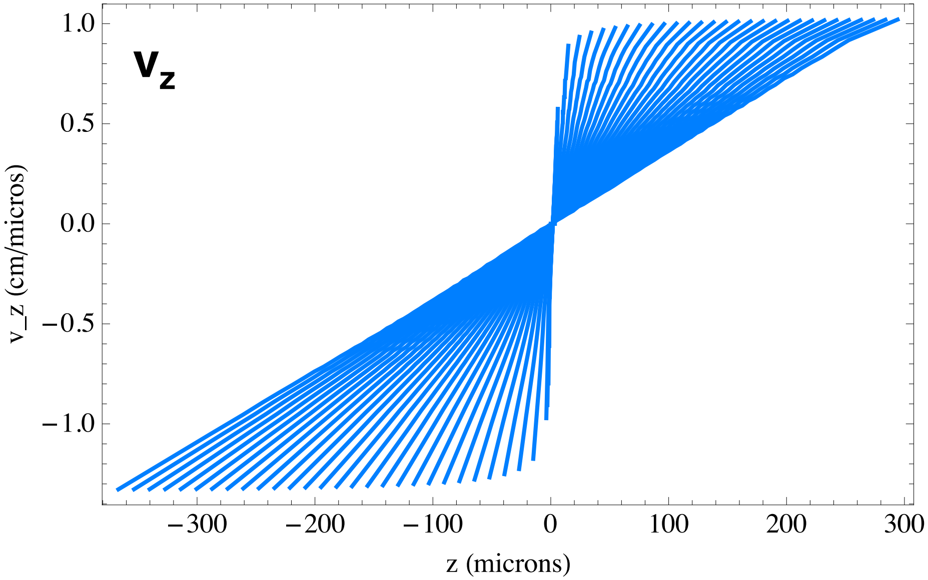

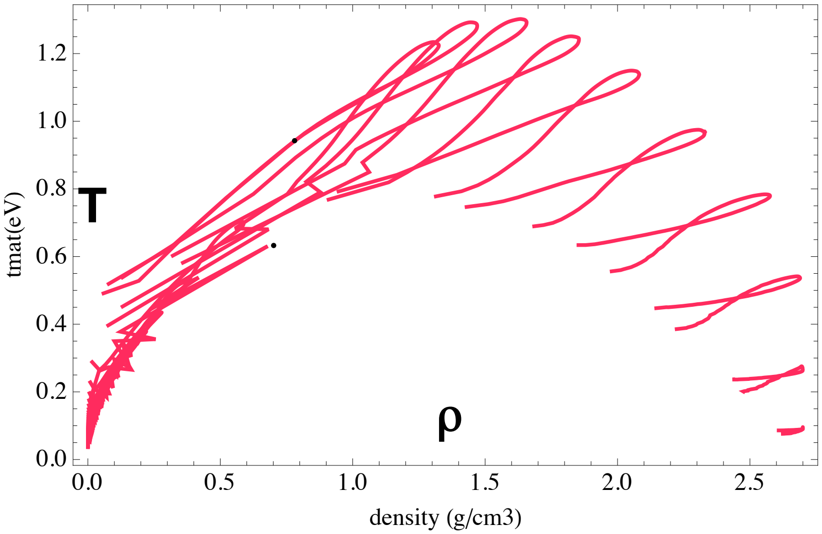

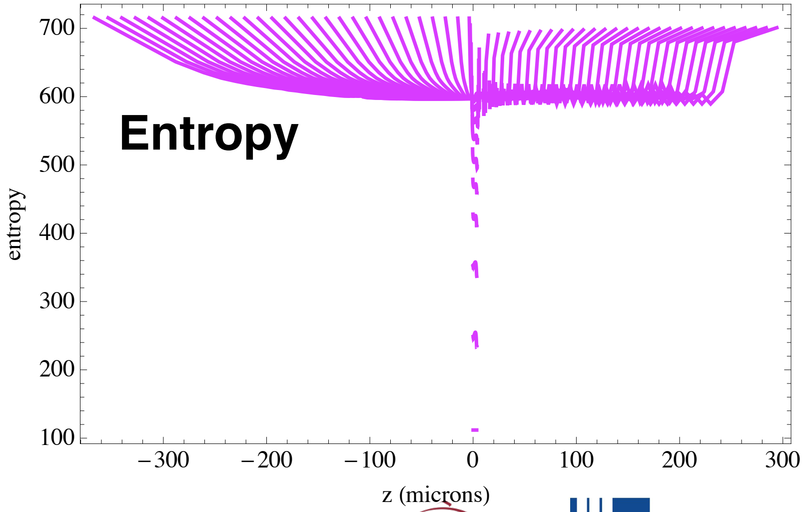

Critical frequency ν_{crit} defines "over dense" point where wave propagation becomes evanescent

$$h\nu_{crit} = h\omega_p/2\pi = 28\ \text{eV}\ \sqrt{\rho(\text{g/cm}^3)Z^*/\text{A}_{\text{target}}}$$

Consider idealized case: Energy instantaneously deposited; ideal gas; Z* = constant

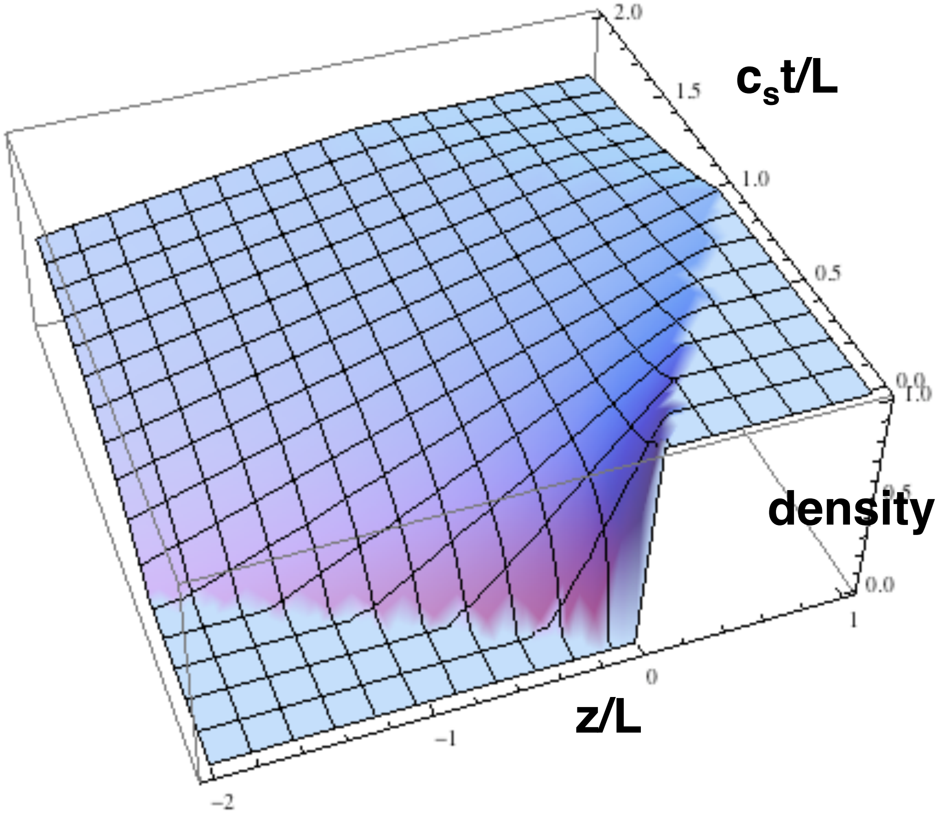

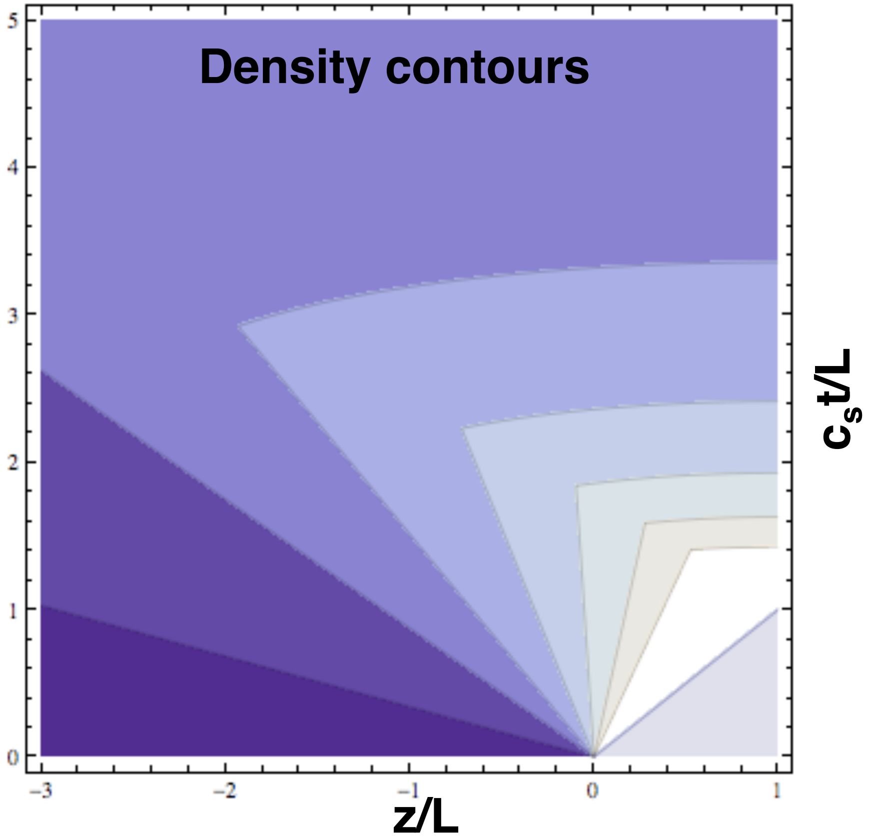

For adiabatic evolution lines of constant density coincide with lines of constant temperature (since T ~ $\rho^{\gamma-1}$).

As estimate of brightness temperature T_b at a given ν we may take the black body intensity at the temperature of the critical point

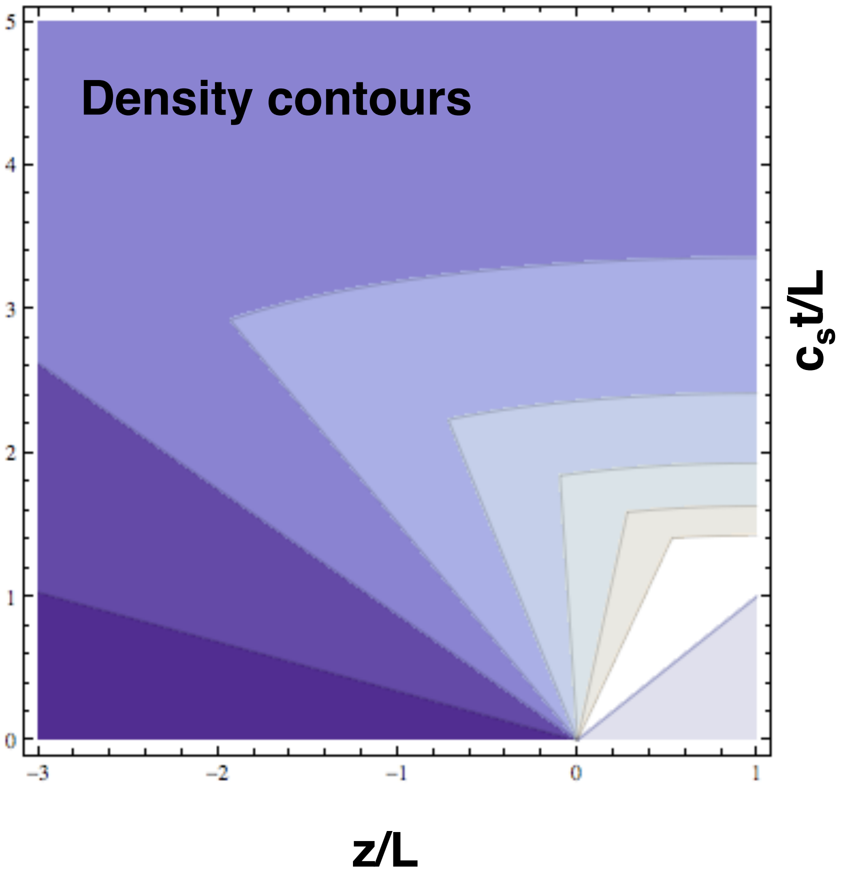

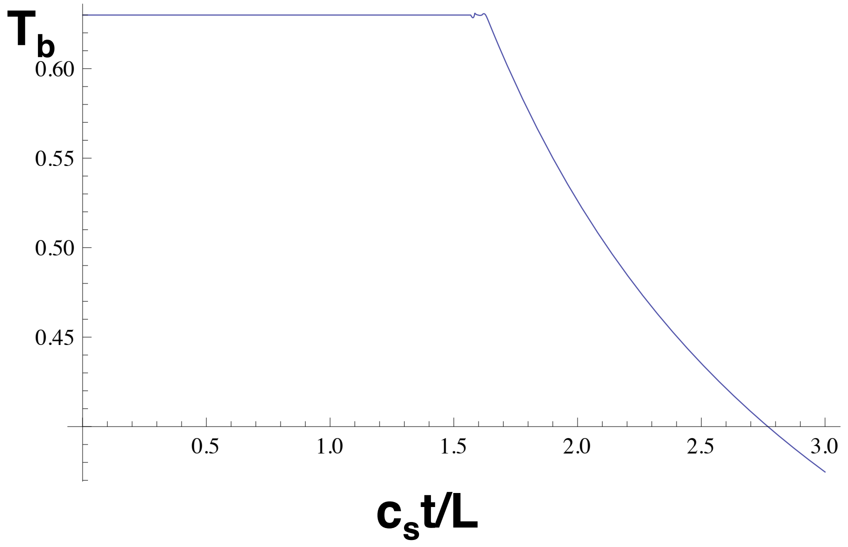

- **Brightness temperature will stay constant until contour reaches z axis**
- **Brightness temperature will stay constant for longer times at lower frequencies**

For the actual target case (QEOS shown here) we may plot $h\nu_{crit}$ vs z and $T(h\nu_{crit})$ vs t for several $h\nu_{crit}$'s

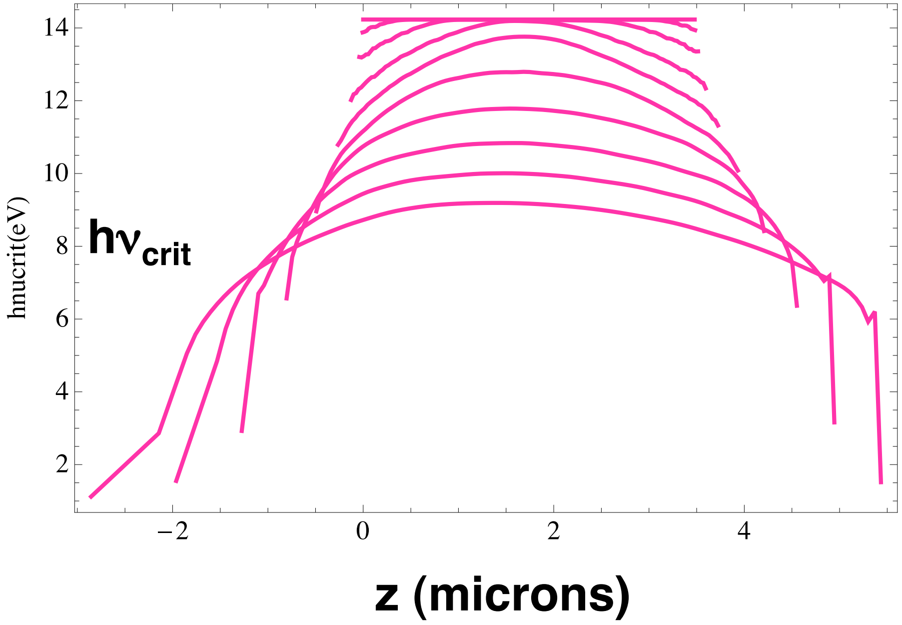

Model assumes:

$T_b = T(h\nu_{crit})$ if $h\nu_{critmin} < h\nu < h\nu_{critmax}$
$T_b = Tmax$ if $h\nu > h\nu_{critmax}$
$T_b = 0$ if $h\nu < h\nu_{critmin}$

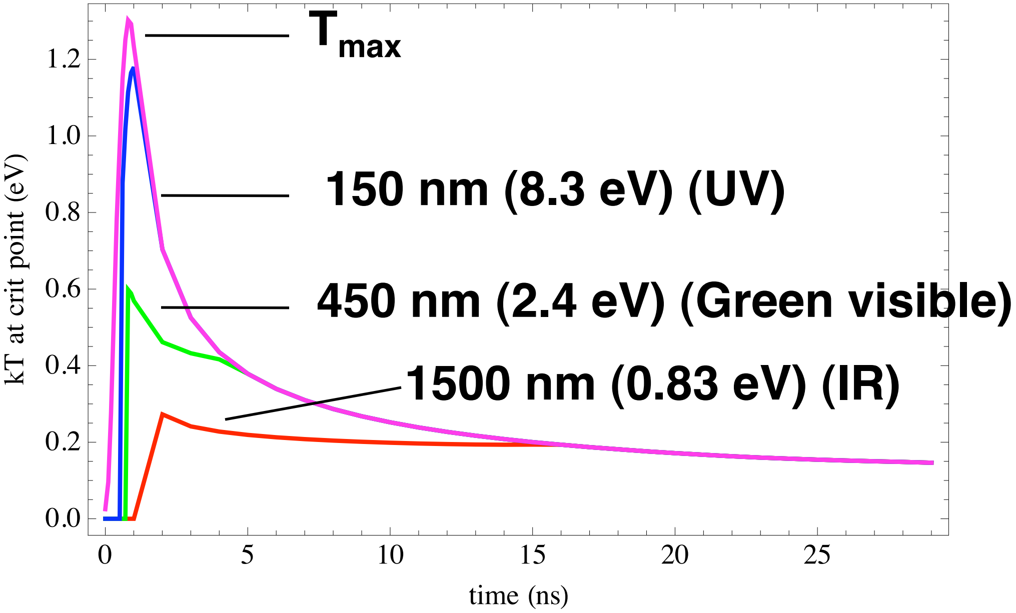

We may compare the same plots for different intensities

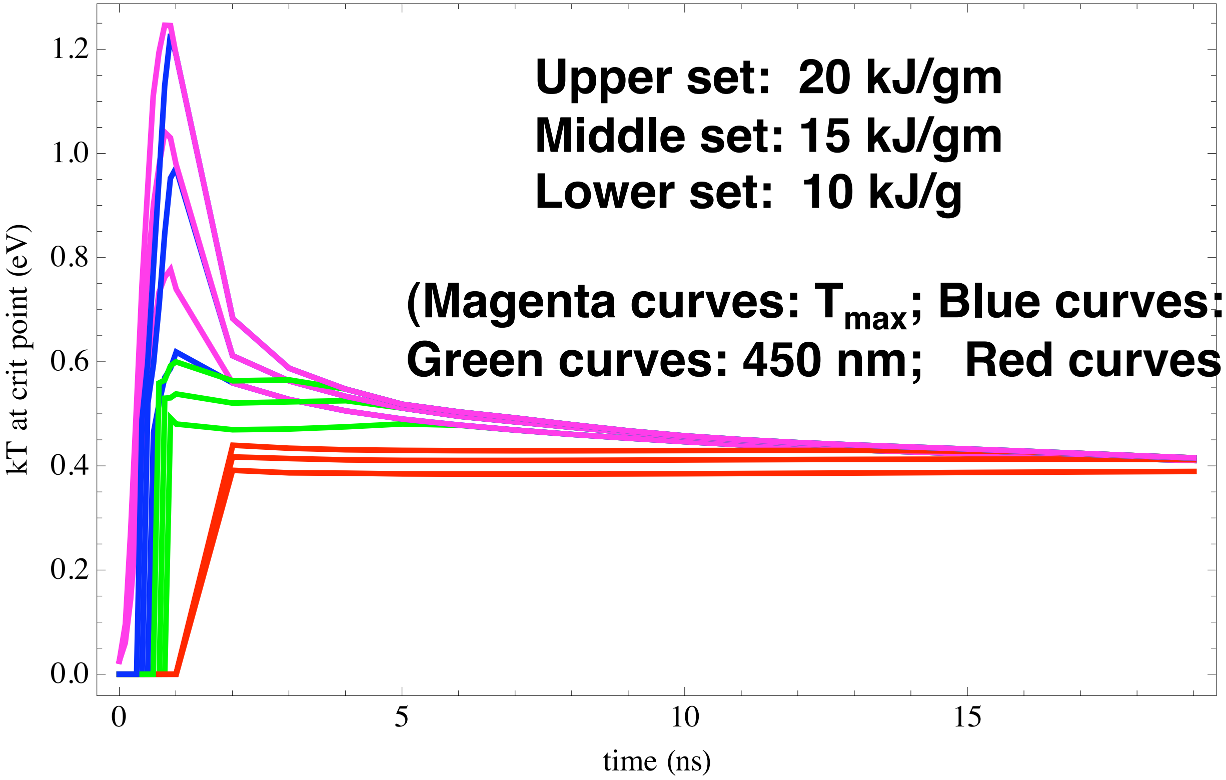

Upper set: 20 kJ/gm
Middle set: 15 kJ/gm
Lower set: 10 kJ/g

(Magenta curves: T_{max}; Blue curves: 150 nm
Green curves: 450 nm; Red curves: 1500 nm)

(UV most sensitive to change in deposited energy;
IR (which samples cooler part of blowoff, less sensitive)

We may also compare two equations of state

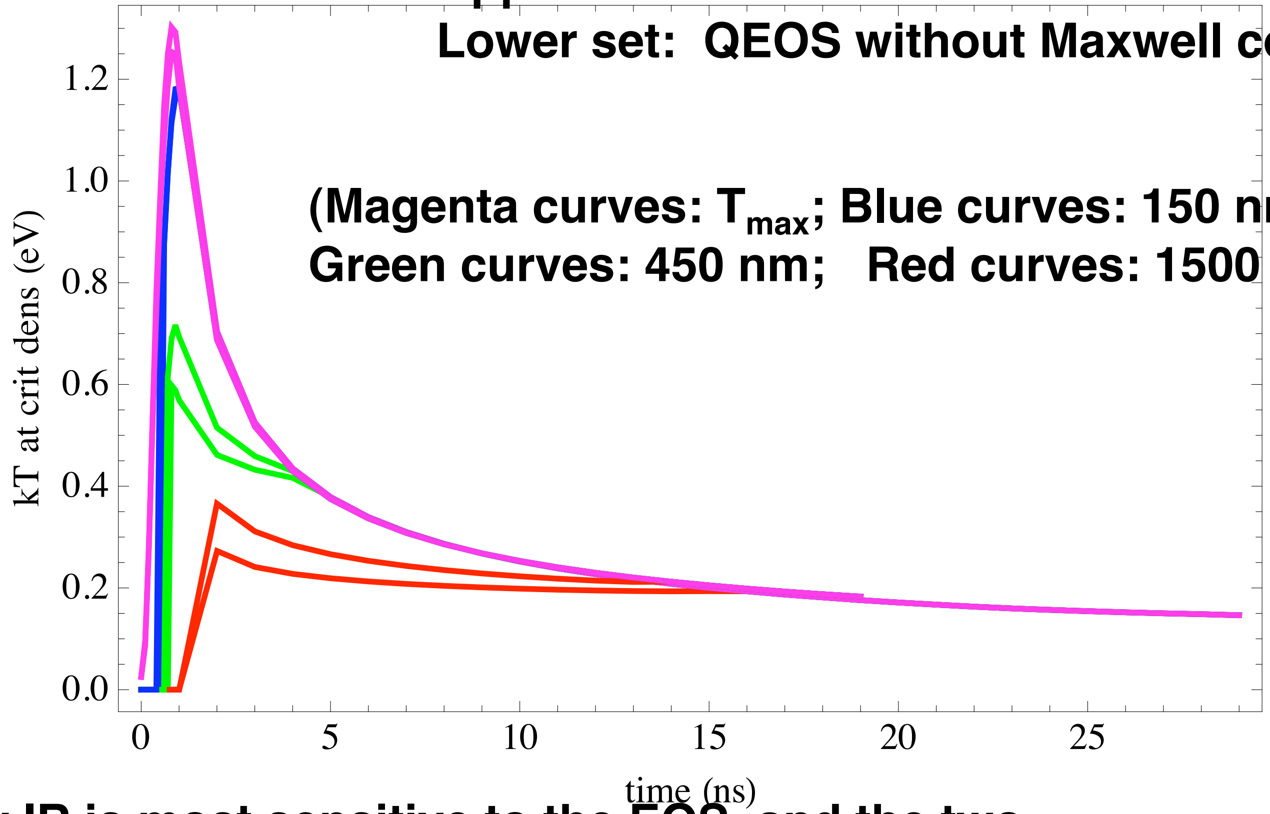

Upper set: LEOS without Maxwell construction
Lower set: QEOS without Maxwell construction

(Magenta curves: T_{max}; Blue curves: 150 nm
Green curves: 450 nm; Red curves: 1500 nm)

Now IR is most sensitive to the EOS, and the two EOS should be distinguishable

We may also compare the same equation of state with or without the Maxwell construction

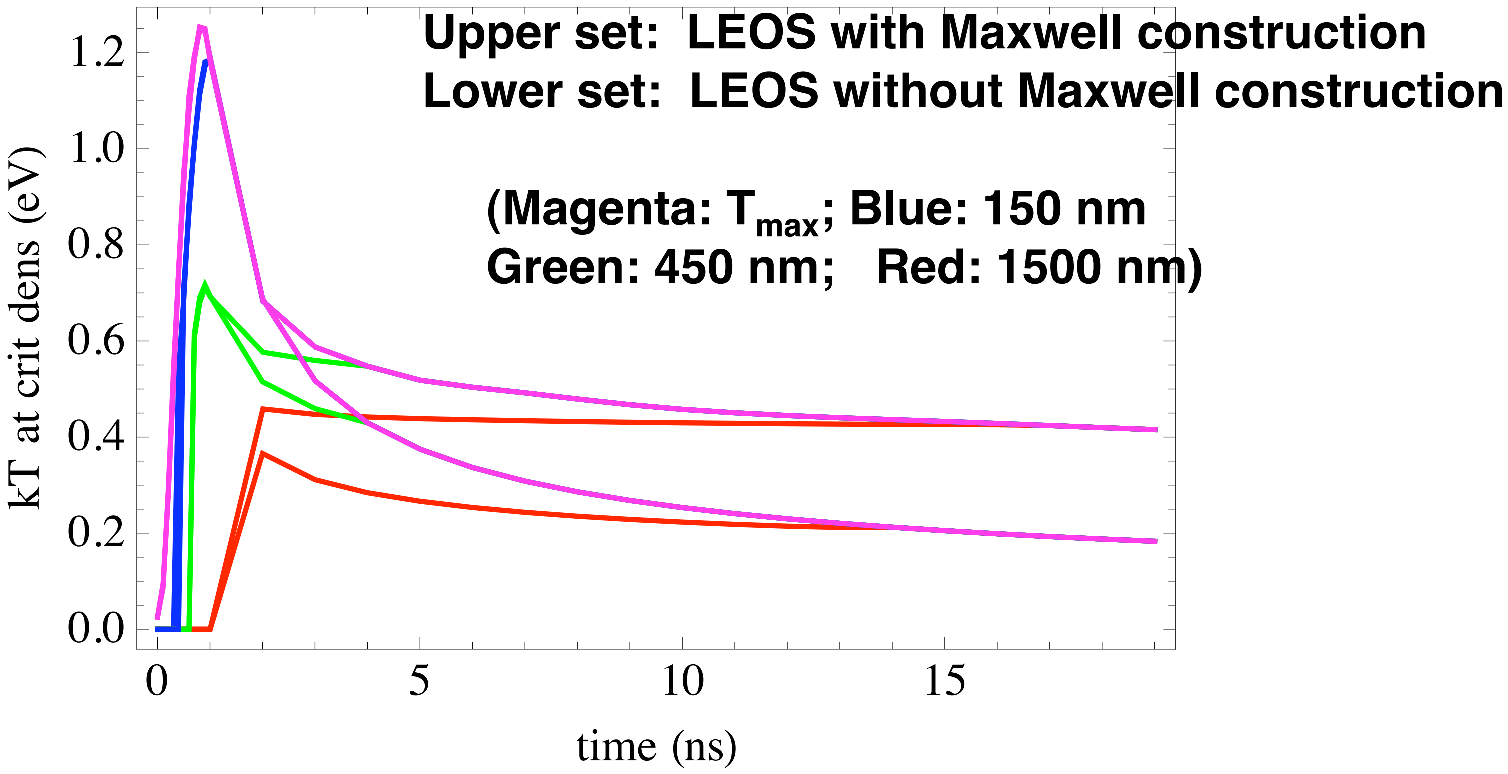

Upper set: LEOS with Maxwell construction
Lower set: LEOS without Maxwell construction

(Magenta: T_{max}; Blue: 150 nm
Green: 450 nm; Red: 1500 nm)

Now IR is VERY sensitive to the choice of Maxwell construction or no Maxwell construction

We may also calculate the velocity at the critical density for a particular photon frequency as a function of time

Again looking at the idealized case (instantaneous heating, ideal gas, constant Z*):

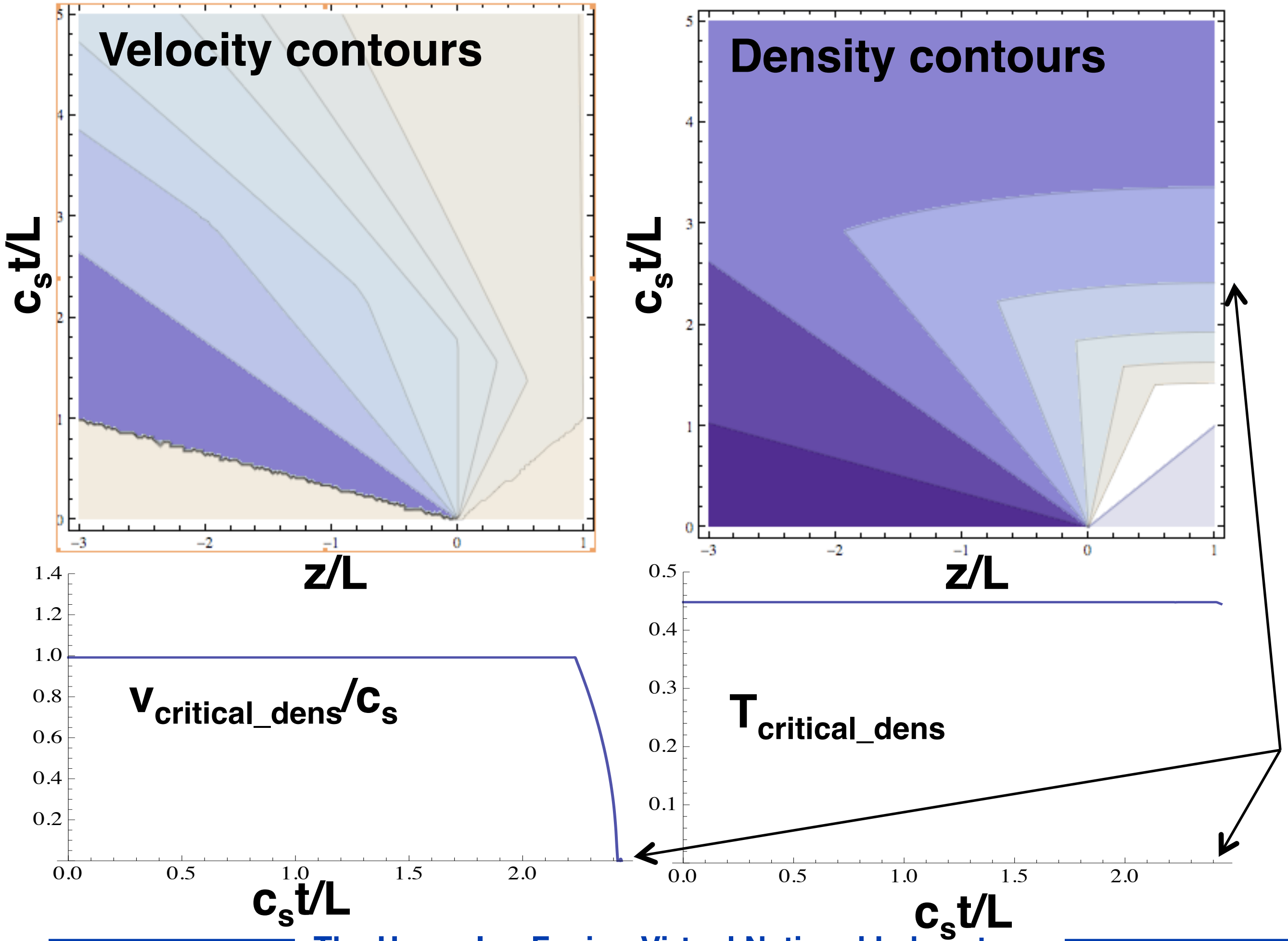

The velocity contours first align with, then cross the density and temperature contours, so the velocity measured at the critical density would first be constant then plummet

Time at which density contour reaches z=0 axis

For realistic equations of state and finite heating time the velocity would also reach zero at the end of the flattop in T_b

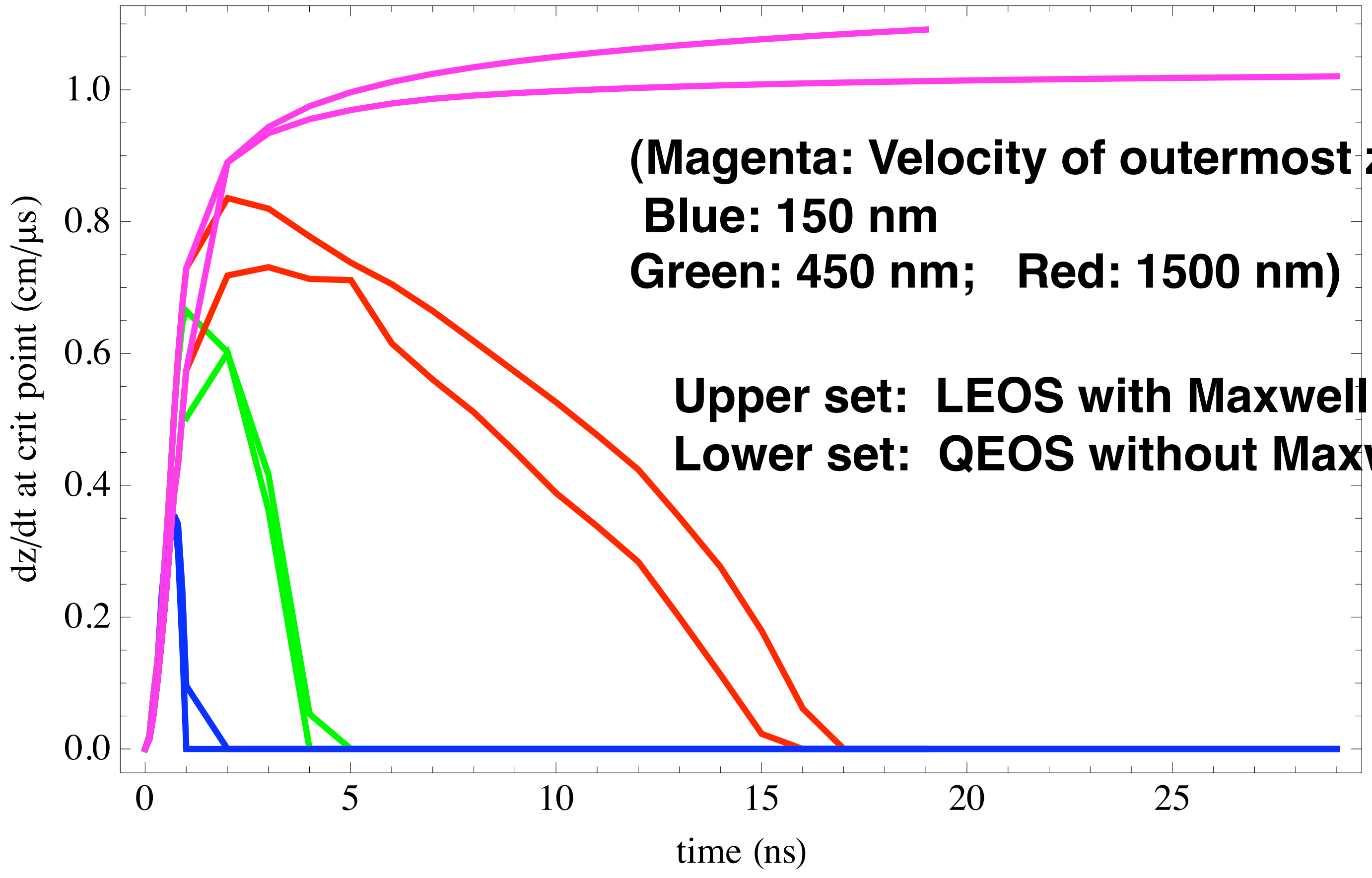

(Magenta: Velocity of outermost zone;
Blue: 150 nm
Green: 450 nm; Red: 1500 nm)

Upper set: LEOS with Maxwell construction
Lower set: QEOS without Maxwell construction

Again, the IR is best suited for distinguishing different EOS

A cylindrical hole can create regions of temperature and pressure larger than in a simple foil

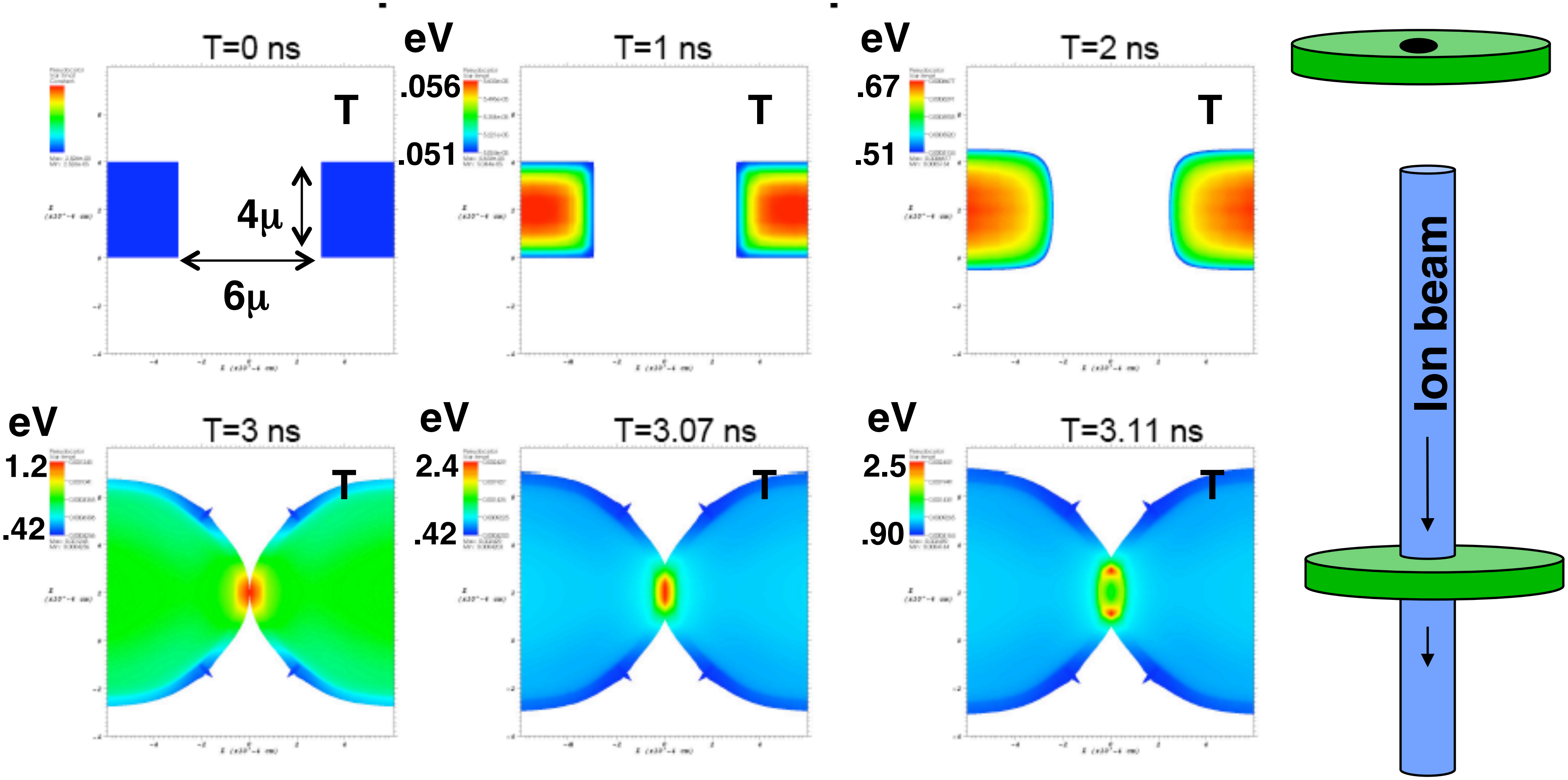

HYDRA simulations by E. Henestroza (using LEOS).

Solid Tin target. 2.8 MeV Li$^+$, 10 J/cm^2 assumed.

T_{max} = 2.6 eV; P_{max} = 1.3 Mbar ρ_{max}= 11 g/cm^3 (ρ_{init}= 7 g/cm^3); v_{imp} = 3.5 km/s

Advantage: relatively easy to manufacture and diagnose

If instead of a cylindrical hole, a spherical void is placed in the foil, higher pressures are possible

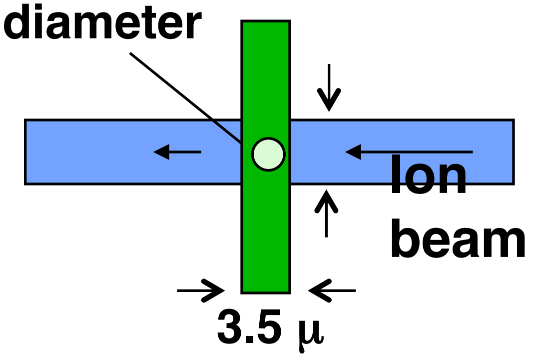

1 μ bubble diameter

Ion beam

3.5 μ

Simulation:

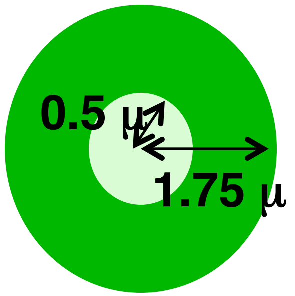

0.5 μ

1.75 μ

Deposition:
25 kJ/g/ns for 1 ns

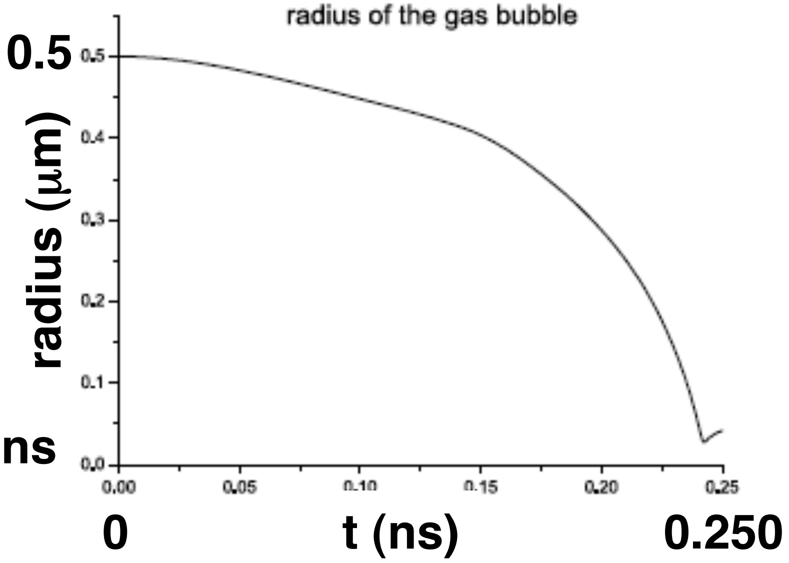

Simulations by Siu-Fai Ng (using DISHr, QEOS)

P_{max} > 10 Mbar, T_{max} > 10 eV, ρ_{max} > 5 g/cm^3

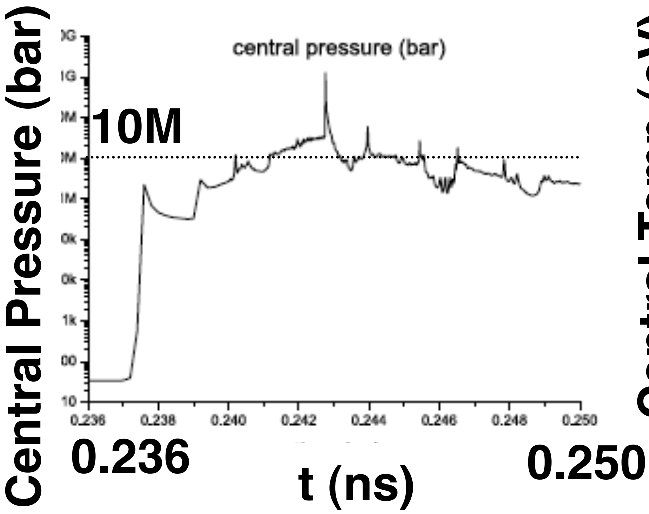

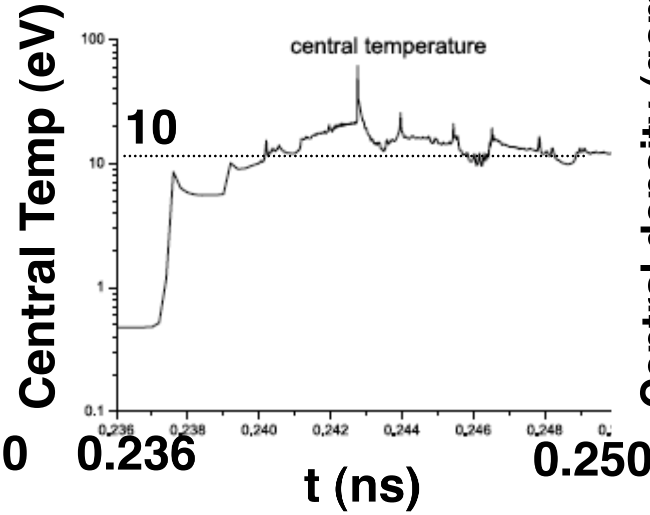

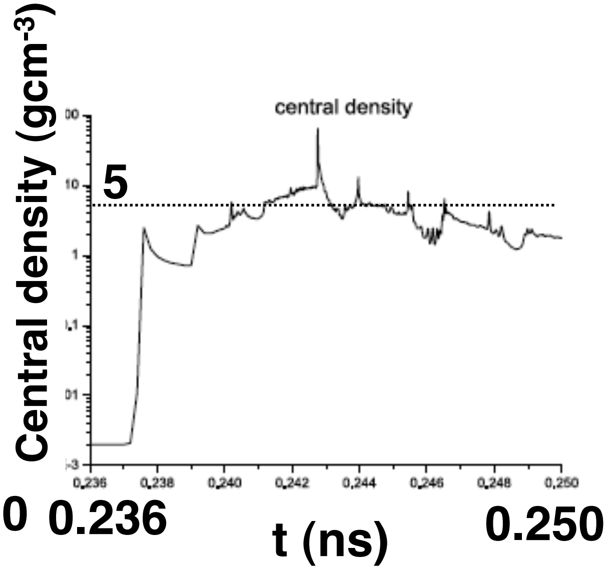

Foams have been modeled as layers of solid separated by layers of void

Codes used on foam modeling include: DPC (Saha based EOS), HYDRA (using QEOS), and DISH (using van der Waals EOS)

Foams of interest because:

1. **Intrinsic physics**
2. **Radiator for HIF**
3. **Structural material in ICF**

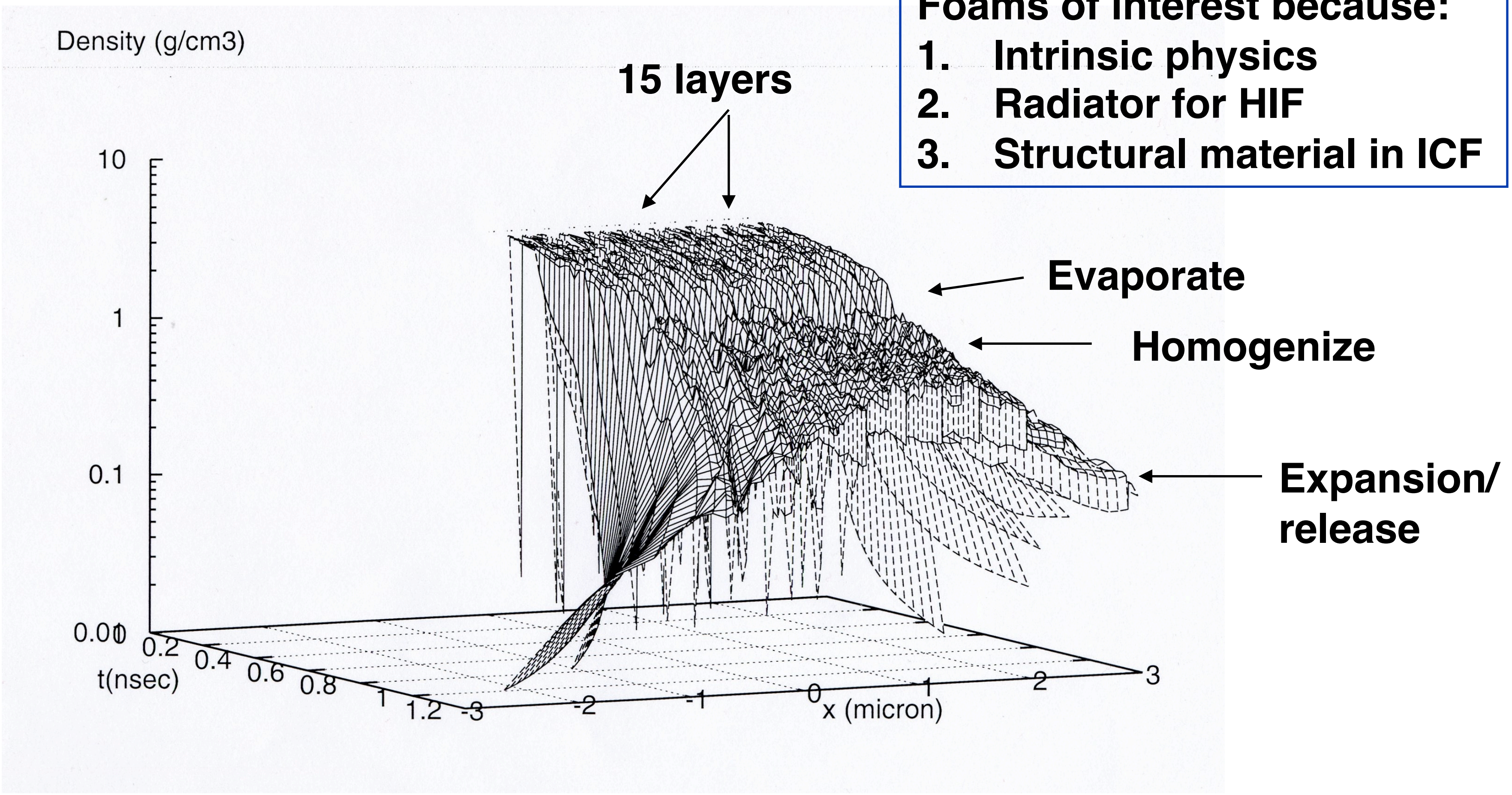

NDCX II will also study ion beam coupling physics that is key to creating high gain direct drive targets for Inertial Fusion Energy

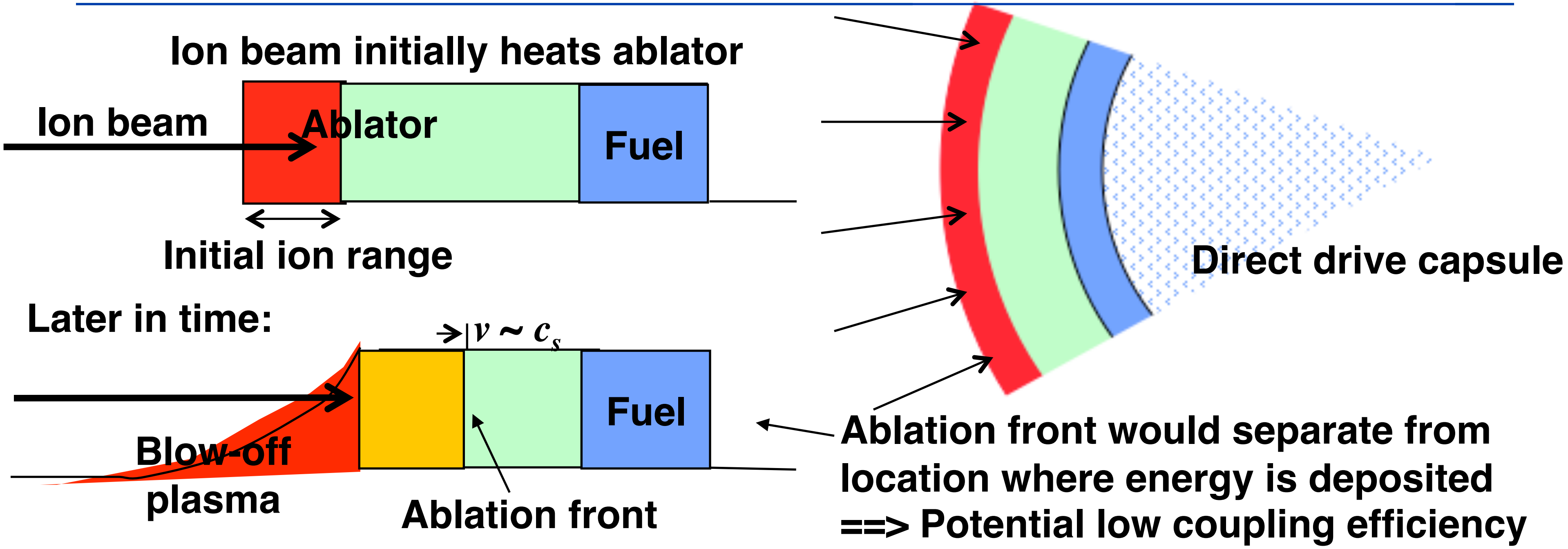

Ion beam initially heats ablator

Ion beam

Ablator

Fuel

Initial ion range

Later in time:

$v \sim c_s$

Fuel

Blow-off plasma

Ablation front

Direct drive capsule

Ablation front would separate from location where energy is deposited ==> Potential low coupling efficiency

Unique features of heavy ion direct drive can maximize drive efficiency:

1. Passive approach: Ion beam heating causes electron thermal speed to go above ion velocity ==> range lengthens, and ion beam can stay close to ablation front, (if ion energy is sufficiently low)

2. Active approach: Ramping ion beam energy over the course of the pulse, will also increase range.

Recent heavy ion capsule designs by Perkins show NIF target yields at 1/4 to 1/3 the driver energy of NIF

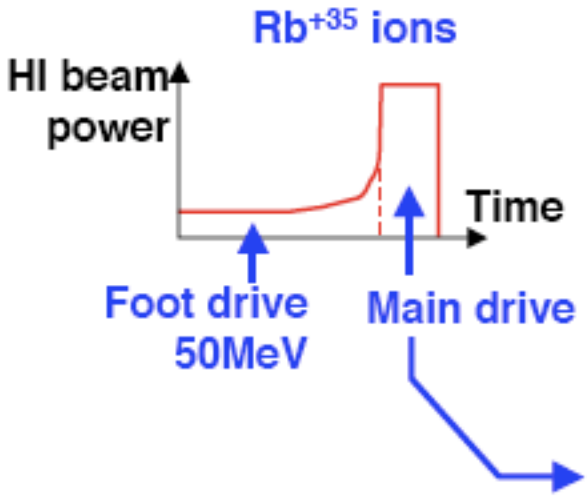

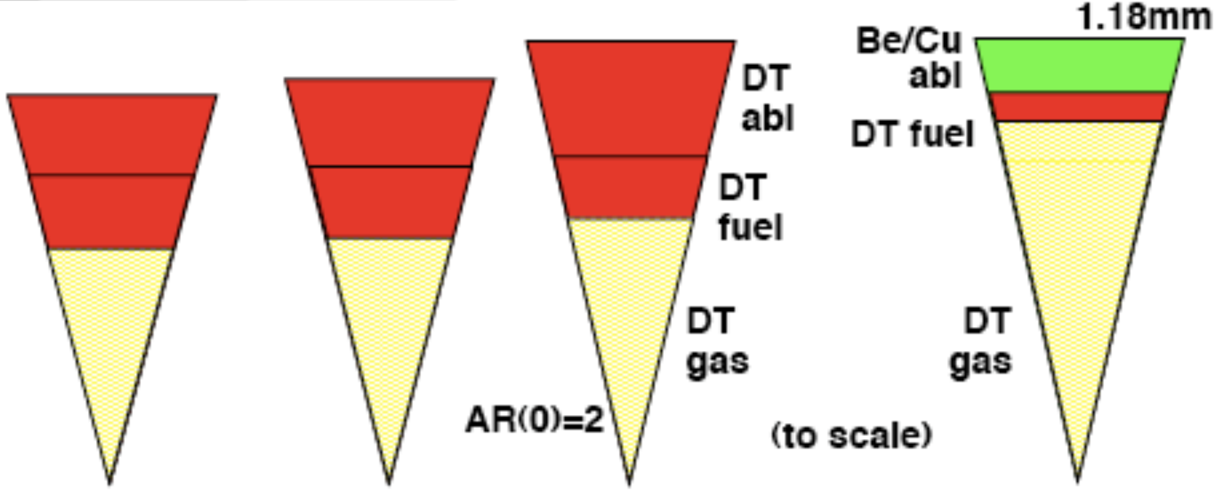

	50MeV	200MeV	500MeV	NIF
$m_{ablator}/m_{fuel}$	1.8	2.1	3.0	18
Driver energy (MJ)	0.32	0.36	0.44	1.3
Peak drive power (TW)	175	195	205	320
Yield (MJ) / Gain	24.7 / 77	21.6 / 60	20.8 / 47	20.0 / 15
$\eta_{absorbed} / \eta$	0.97 / 0.10	0.91 / 0.10	0.88 / .09	0.16 / 0.02
In-flight aspect ratio	25	27	25	32
Convergence ratio	35	30	31	34
In-flight adiabat α	1.9	2.4	3.2	1.4

(from J. Perkins et al, Hirschegg Presentation, 2009).

Conclusions

NDCX II is being designed for both Warm Dense Matter (WDM) and Heavy Ion Fusion (HIF) applications

For WDM, several target geometries lead to warm dense matter conditions

- planar targets at ~ 1 eV, .5 MBar are predicted;
- cylindrical imploding bubbles will reach a few eV, 1 MBar
- spherical imploding bubbles can reach ~10 eV, 10 Mbar

Foam dynamics are of interest for both WDM and HIF applications.

NDCX II pyrometry experiments should relatively easily be able to distinguish between specific equations of state (for example, QEOS and LEOS). VISAR experiments may also be able to distinguish different EOS.

For HIF, we are exploring direct drive concepts that have high coupling efficiency, by utilizing temperature dependent range and ramped ion energy. NDCX II will be able to test key aspect of direct drive target concept: changing ion energy to keep ion deposition point close to ablation front. Beam physics such as wobbler, and beaming bending can be tested.